

# Scaling of Einstein-Podolsky-Rosen steering in spin chains

**W. W. Cheng**

Turku Centre for Quantum Physics, Department of Physics and Astronomy, University of  
Turku, FI-20014 Turun yliopisto, Finland  
Institute of Signal Processing & Transmission, Nanjing University of Posts and  
Telecommunication, Nanjing 210003, China

**J. Piilo**

Turku Centre for Quantum Physics, Department of Physics and Astronomy, University of  
Turku, FI-20014 Turun yliopisto, Finland

E-mail: wcheng@njupt.edu.cn

**Abstract.** Symmetric quantum properties and correlations have been often used earlier to study quantum phase transitions in many body systems and spin models. However, the use of asymmetric quantum features, such as steering, have attracted smaller amount of attention in this context, so far. We study EPR steering and quantum phase transitions in the Ising model in transverse field and in the anisotropic  $XY$  model by using steering robustness and quantum renormalization group method. The key ingredients of the quantum criticality near the critical points, such as finite-size scaling behaviour and critical exponents, are investigated in detail with two commonly used spin models. Our results show that the first derivative of steering robustness between two blocks diverges near the quantum phase transition points for both models, and exhibits a finite-size scaling effect. Moreover, we explore in detail the asymmetric character of EPR steering, by taking into accounts finite-size effects and measurement number, in the reduced block state in the anisotropic  $XY$  model. The results imply that one-way EPR steering does not exist in large system under the limit  $L \rightarrow \infty$  despite the fact that EPR steering for the reduced block state is asymmetric.

PACS numbers: 03.65.Ta, 75.10.Jm, 03.65.Ud

Submitted to: *Phys. Scr.*

## 1. Introduction

Einstein-Podolsky-Rosen steering refers to an ability that one observer, by making local measurements, can change in nonlocal manner (i.e., steer) the quantum state of other observer in remote location. Although this concept was proposed by Schrödinger as response to EPR paradox near century years ago, there does not exist a rigorous definition until Wiseman, Jones and Doherty formalized such issue in an operational way within the quantum information task framework in 2007 [1]. Moreover, they showed that there exists a rigid hierarchy among different quantum nonlocality (i.e., all Bell nonlocal states are contained in steering states, and all steering states are contained in entangled states) [1, 2]. Indeed, one of the most distinguishing features of EPR steering is that it exhibits an intrinsic asymmetry between the two observers, Alice and Bob [1, 2, 3]. In other words, Alice may steer Bob's state, but it may be not possible for Bob to steer Alice's state for a given entangled state shared by the two observers (i.e., one-way EPR steering). In the past years, this concept has attracted flourishing attention in many branches of physics both for theoretical and experimental aspects [4, 5, 6, 7, 8, 9, 10, 11, 12, 13, 14, 15, 16, 17, 18, 19, 20, 21, 22, 23, 24] due to its potential applications in practical quantum information processing, such as entanglement-assisted subchannel discrimination [10], the quantum key distribution [14], randomness generation [17] and secure teleportation [18].

On the other hand, quantum correlations not only are fundamental to numerous applications of quantum information processing, but also are essential elements of the many-body physics. For instance, many recent works show that there exist a close relationship between quantum correlations and the emergence of the quantum phase transition (QPT) in many-body systems [25]. And such connections have been studied from many different perspectives in varying quantum spin systems and chains [26, 27, 28, 29, 30, 31, 32, 33, 34, 35, 36, 37, 38, 39]. Entanglement and Bell nonlocality, as two typical quantum nonlocality, have been employed to characterize the QPT [26, 27, 28, 29, 30, 31, 32, 33, 34, 35, 36]. The results indicate that quantum correlations are indeed a useful and nontrivial tool to characterize the QPT of a quantum system. However, in most of the previous works, only symmetric quantum correlations (e.g., entanglement and Bell nonlocality) have been utilized as an information-theoretic tool to estimate the critical properties in the spin systems whilst asymmetric correlations, such as steering,

has so far rarely been considered in this context. This motivates us to use EPR steering for the studies of quantum criticality in the spin systems and in particular focus on the following questions. Do there exist the finite-size scaling effect for EPR steering in the critical system? And whether can we estimate accurately the critical exponent of correlation length by investigating quantum steering? Combining with the quantum renormalization group (RG) method in the Ising model in the transverse field (ITF) and the  $XY$  model, we present some results for the above questions in this work. We explore the nonanalytic behaviour and scaling effect for the EPR steering in detailed manner. Furthermore, we study the asymmetry properties of EPR steering between the two observers in the reduced block state by taking account both the number of measurements and finite-size effects.

This article is organized as follows. In the section 2, we give a brief introduction to EPR steering and its measurement. In Section 3 and 4, we carry rigorous study to understand the features of the EPR steering and the quantum critical properties in ITF model and  $XY$  one, respectively. In Section 5, the asymmetric character of EPR steering is explored under different measurements and system size  $L$ . Finally, Section 6 summarizes our main results.

## 2. EPR Steering and its measurement

Consider two remote observers, Alice and Bob, sharing a bipartite quantum entangled state  $\rho_{AB}$ . One of them (e.g., Alice) can choose to perform measurement on her subsystem, described by operators  $\{M_{a|x}\}$  satisfying  $M_{a|x} \geq 0$  and  $\sum_a M_{a|x} = I$  (Here,  $x$  and  $a$  denote the measurement setting and the corresponding outcome, respectively). Then, the possible Bob's states, which depend on Alice's measurement  $x$  and the corresponding output  $a$ , can be characterized by a collection (or assemblage) of density matrices  $\{\sigma_{a|x}\}_{a,x}$  as follows,

$$\sigma_{a|x} = \text{Tr}_A(M_{a|x} \otimes I \rho_{AB}). \quad (1)$$

Here, it should be mentioned that the collection  $\{\sigma_{a|x}\}_{a,x}$  must satisfy two conditions simultaneously: no-signaling requirement

$$\sum_a \sigma_{a|x} = \sum_a \sigma_{a|x'} \quad \forall x, x' \quad (2)$$

and normalization one

$$\text{tr} \sum_a \sigma_{a|x} = 1 \quad \forall x, \quad (3)$$

respectively. Now, according the definition of quantum steering proposed by Wiseman et al. (i.e., the possibility of the remotely generating ensembles  $\{\sigma_{a|x}\}_{a,x}$  could be reproduced by a local hidden state (LHS) model [1, 2]), we call an assemblage  $\{\sigma_{a|x}\}_{a,x}$  unsteerable if all elements in the collection can be written in the form

$$\sigma_{a|x} = \sum_{\xi} D_{\xi}(a|x) \sigma_{\xi} \quad \forall a, x \quad (4)$$

with condition

$$\text{tr} \sum_{\xi} \sigma_{\xi} = 1, \quad \sigma_{\xi} \geq 0 \quad \forall \xi. \quad (5)$$

We denote it as  $\{\sigma_{a|x}^{US}\}_{a,x}$ . Otherwise, we call any assemblage  $\{\sigma_{a|x}\}_{a,x}$  that cannot be written in the above expression steerable, and such kind of assemblage is marked by  $\{\sigma_{a|x}^S\}_{a,x}$ . Here,  $\xi$  is a classical local hidden variable, which shows the correlations between Alice's and Bob's measurement results that can be explained under the frame of classical realism. By using semi-definite program (SDP) [5, 6, 7, 8], one can judge which kinds of assemblage should be belonged for a given collection  $\{\sigma_{a|x}\}_{a,x}$  straightly.

Another interesting and important question is how to quantify EPR steering and recently several scenarios have been proposed for this purpose. Combining with the semi-definite program and decomposing an assemblage into two parts (i.e.,  $\sigma_{a|x} = \mu \sigma_{a|x}^{US} + (1 - \mu) \sigma_{a|x}^S$ ,  $\forall a, x$ ,  $0 \leq \mu \leq 1$ ), Skrzypczyk et al. proposed a concept called steering weight to quantify the steerability for a given quantum assemblages [5]. Then they defined steering weight as  $SW = 1 - \mu^*$  (Here,  $\mu^*$  denotes the maximum  $\mu$  in the decomposition). Along this line, Chen et al. extended this scenario to its temporal analogue, quantum temporal steering [11]. Corresponding to the robustness of entanglement, Piani et al. proposed a new quantity called steering robustness  $\mathcal{R}$  from an altering approach by asking how much mixing must one add to a given assemblage  $\{\sigma_{a|x}\}_{a,x}$  in order for it to be explained by locally hidden state model [10]. Generally, a  $\mathcal{N}$ -robustness of an assemblage  $\{\sigma_{a|x}\}_{a,x}$  can be defined as [6, 10],

$$\begin{aligned} \mathcal{R}(\sigma_{a|x}) &= \min_{\sigma_{a|x}, \sigma_{\lambda}, t} t \quad s.t. \\ \frac{\sigma_{a|x} + t \tau_{a|x}}{1 + t} &= \sigma_{a|x}^{LHS} \quad \forall a, x \\ \sigma_{a|x}^{LHS} &= \sum_{\lambda} D(a|x, \lambda) \sigma_{\lambda} \quad \forall a, x \\ \tau_{a|x} &\in \mathcal{N}, \sigma_{\lambda} \geq 0 \quad \forall \lambda. \end{aligned} \quad (6)$$

Here,  $\mathcal{N}$  is any subset of assemblages characterized by positive semi-definite constraints and linear matrix inequalities. The values of  $\mathcal{R}$  means the minimal "noise" to destroy the steerability for a given assemblage (or corresponding quantum state  $\rho$ ). We can find the value of  $t \simeq 0.27$  for the Bell state, whereas no mixing needs be added ( $t = 0$ ) for the product state. Here, it should be mentioned that steering robustness measure  $\mathcal{R}$  seems to be finer than the steering weight due to the fact that all

pure entangled states are maximally steerable (i.e., steering weight equal to one) [5], but it is not maximal for steering robustness. For instance, pure state  $|\chi\rangle = \sqrt{1 - \alpha^2}|00\rangle + \alpha|11\rangle$  ( $-1 < \alpha < 1$ ) has maximum steering weight 1 even under the extreme condition  $\alpha \rightarrow 0$  or  $|\alpha| \rightarrow 1$ . However, the amount of noise that need to be added to this pure state to have nonsteerable assemblages is very small and steering robustness  $\mathcal{R}$  for this state is very close to zero under the condition  $\alpha \rightarrow 0$  or  $|\alpha| \rightarrow 1$  [13]. Thereby we will take steering robustness  $\mathcal{R}$  as a measure in the following study.

### 3. EPR steering in ITF model

First, we study EPR steering in the ITF model. The Hamiltonian of such model for  $L$  qubits can be written as

$$H(J, \lambda) = -J \sum_i^L (\sigma_i^z \sigma_{i+1}^z + \lambda \sigma_i^x). \quad (7)$$

$J$  and  $\lambda$  denote the exchange interaction and the transverse field strength, respectively. This model can be solved exactly by transforming the spin operators to free fermions in terms of the Jordan-Wigner transformation [27, 28]. Here, we study EPR steering and QPT in this model by exploiting the quantum RG method [29, 31].

Renormalization group is a standard mathematical tool that allows systematic investigation of the changes of a physical system as viewed at different distance scales. The main objective of the RG method is to eliminate the effective degrees of freedom of the system via a recursive procedure until a mathematically tractable situation is reached. Commonly, the original Hamiltonian  $H$  can be decomposed into two parts by taking the Kadanoff's block method (i.e., the block part Hamiltonian  $H^B$  and inter-block part Hamiltonian  $H^{BB}$ ). Then the low-lying eigenstates (e.g. ground states) of the block Hamiltonian can be obtained exactly by solving the eigenvalues equation  $H^B|\psi\rangle = E|\psi\rangle$ . Subsequently, we can construct the bias for the renormalized space by using the above low-lying eigenstates. Thereby, an effective Hamiltonian can be achieved by projecting the full Hamiltonian onto the renormalized space. Interesting, we can find that the structure of effective Hamiltonian is very similar with the original ones.

For the above ITF model, we can decompose the original Hamiltonian into the block parts  $H^B$  and the interacting parts  $H^{BB}$  respectively as follows [29, 31],

$$\begin{aligned} H^B &= -J \sum_I^{L/2} (\sigma_{I,1}^z \sigma_{I,2}^z + \lambda \sigma_{I,1}^x) \\ H^{BB} &= -J \sum_I^{L/2} (\sigma_{I,2}^z \sigma_{I+1,1}^z + \lambda \sigma_{I,2}^x). \end{aligned} \quad (8)$$

Here,  $\sigma_{I,j}^{\alpha}$  denote the Pauli operators at site  $j$  of the  $I$ th block. By solving the Schrödinger equation  $-J(\sigma_{I,1}^z \sigma_{I,2}^z +$

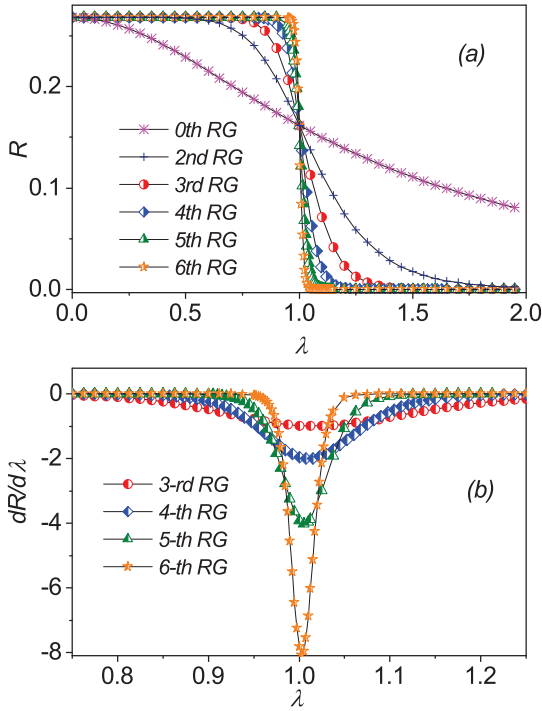


**Figure 1.** (Color online) (a) Steering robustness  $\mathcal{R}$  of the ITF chain with respect to  $\lambda$  under different  $n$ th RG. (b) Evolution of the first derivative of steering robustness  $d\mathcal{R}/d\lambda$  at different RG steps. Hereafter, we set three types of measurements corresponding to the projections on the eigenstates of the three Pauli operators  $X$ ,  $Y$  and  $Z$  without additional remark [11].

$\lambda\sigma_{i,1}^x|\varphi\rangle = E|\varphi\rangle$ , we can easily obtain the two degeneracy ground states as follows,

$$\begin{aligned} |\varphi_0\rangle &= \alpha|00\rangle + \beta|11\rangle \\ |\varphi'_0\rangle &= \alpha|01\rangle + \beta|10\rangle. \end{aligned} \quad (9)$$

Here, the coefficients  $\alpha = s/\sqrt{s^2+1}$ ,  $\beta = 1/\sqrt{s^2+1}$  and  $s = \sqrt{\lambda^2+1} + \lambda$ . By using the projection operator  $P_0^I = |\uparrow\rangle\langle\uparrow| + |\downarrow\rangle\langle\downarrow|$  ( $|\varphi_0\rangle$  and  $|\varphi'_0\rangle$  are the above two degeneracy ground states), the relations between the original Hamiltonian and the renormalized one can be formulated as follows

$$H^{eff} = P_0(H^B + H^{BB})P_0. \quad (10)$$

By a straightly calculation, one can obtain an effective Hamiltonian of the renormalized chain as follows,

$$H^{eff} = -J' \sum_i^{L/2} (\sigma_i^z \sigma_{i+1}^z + \lambda' \sigma_i^x), \quad (11)$$

which is exactly similar to the original one. Here, the coefficients  $J'$  and  $\lambda'$  in the effective Hamiltonian satisfy the following iterative relationship,

$$J' = J \frac{2(\sqrt{\lambda^2+1} + \lambda)}{1 + (\sqrt{\lambda^2+1} + \lambda)^2}, \quad \lambda' = \lambda^2. \quad (12)$$

Above iterative relationship, associated with the quantum RG process, contain the important information,

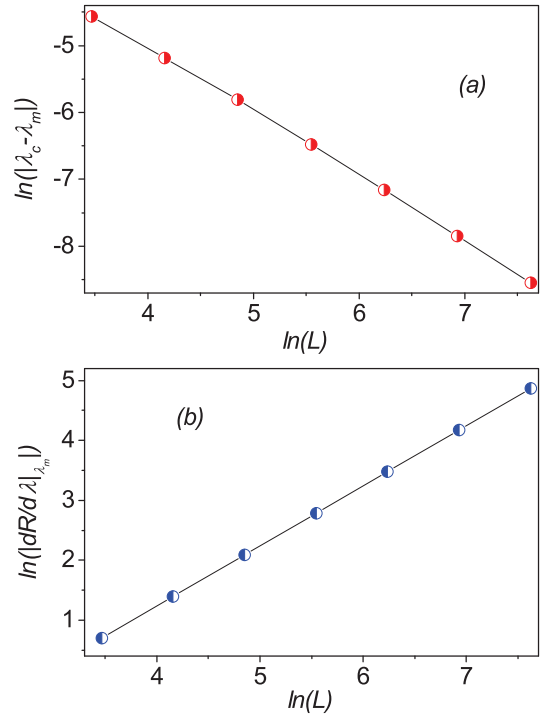


**Figure 2.** (Color online) (a) The distance between the position of pseudo-critical point  $\lambda_m$  and the real one  $\lambda_c$  with respect to different system size  $L$  ( $n$ th RG).  $\lambda_m$  approaches to  $\lambda_c$  in terms of  $\lambda_m = \lambda_c + L^{-0.96 \pm 0.01}$ . (b) The minimum of the first derivative of steering robustness  $d\mathcal{R}/d\lambda$  with respect to different system size.

e.g., fixed points. By solving the iterative relationship equation  $\lambda' = \lambda^2$ , we can easily obtain two stable fixed points ( $\lambda = 0$  and  $\lambda = \infty$ ) and one unstable fixed point ( $\lambda = 1$ ). Roughly speaking, the phase diagram can be obtained by analyzing these points due to the facts that stable fixed points correspond to the stable phases and unstable fixed ones locate at the boundary between different stable phases for a given model. In the current case, the stable phases are characterized by two fixed points  $\lambda = 0$  (corresponding to long-ranged ordered Ising phase) and  $\lambda = \infty$  (corresponding to the paramagnetic phase), respectively. The critical point ( $\lambda_c = 1$ ) locates at the boundary between the Ising phase  $\lambda < \lambda_c$  and paramagnetic ones  $\lambda > \lambda_c$ . In the previous works, some other quantum correlations have been employed to investigate the critical behavior in this model, e.g, entanglement [29], quantum discord, Bell nonlocality, and quantum deficit [31]. It is shown that the first derivative of all these quantum correlations diverge at  $\lambda_c = 1$ , thus can mark the quantum criticality in this model.

By using the pure two-site block quantum state  $|\varphi_0\rangle$ , the density matrix of the block state can be written as

$$\rho = |\varphi_0\rangle\langle\varphi_0| = \begin{pmatrix} \beta^2 & 0 & 0 & \alpha\beta \\ 0 & 0 & 0 & 0 \\ 0 & 0 & 0 & 0 \\ \alpha\beta & 0 & 0 & \alpha^2 \end{pmatrix}. \quad (13)$$

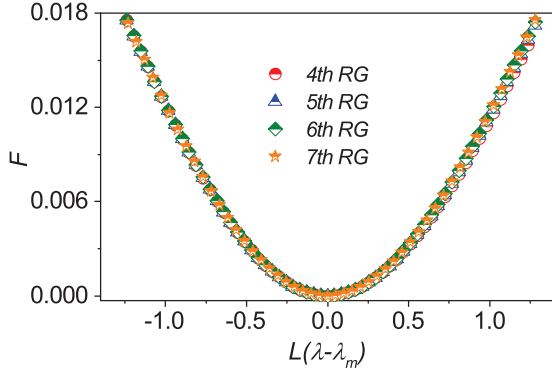


**Figure 3.** (Color online) The evaluated  $F = L^{-1}(\frac{dR}{d\lambda} - \frac{dR}{d\lambda}|_{\lambda_m})$  with respect to  $L(\lambda - \lambda_m)$  for different RG steps  $n = 4, 5, 6$  and  $7$ , all the data for different RG steps almost collapse on a single curve.

In Fig.1(a), we plot the value of  $\mathcal{R}$  with respect to  $\lambda$  for different RG steps. Obviously, all curves of steering robustness  $\mathcal{R} \sim \lambda$  cross each other around the critical point ( $\lambda_c = 1$ ). In comparison with the other quantum correlations demonstrated in previous works [29, 31], steering robustness  $\mathcal{R}$  also develops asymptotically two fixed values:  $\mathcal{R}$  approaches to its maximum asymptotically in the Ising phase ( $\lambda < \lambda_c$ ) and reaches to zero in the paramagnetic phases ( $\lambda > \lambda_c$ ), respectively. This trend becomes more obvious with an increasing system size  $L$ . Furthermore, the steering robustness  $\mathcal{R}$  around the critical point  $\lambda_c$  is discontinued with respect to  $\lambda$  after enough iteration steps (which represent a large enough system size  $L$ ). As shown in Fig.1(a), the steering robustness  $\mathcal{R}$  jumps from a maximum (around 0.27) to 0 with higher iterations.

To further reflect the trend of steering robustness with increasing system size  $L$  (i.e., higher  $n$ th RG), we analyze the behavior of the first derivative of steering robustness  $d\mathcal{R}/d\lambda$  with respect to  $\lambda$ . The results are shown in Fig.1(b). Obviously,  $d\mathcal{R}/d\lambda$  diverge around the critical point. Although there do not exist real divergence for a finite system size  $L$  (i.e., finite  $n$ th RG), the trend of such behavior become more obvious with increasing the lattice size, which indicate a the finite-size scaling behavior. Along this line, the detailed numerical results indicate that the position of the pseudo-critical point  $\lambda_m$  shifts with increasing system size  $L$  as follows,

$$\ln|\lambda_m - \lambda_c| = k_1 \ln L + const, \quad (14)$$

as displayed in Fig.2 (a). Here, the coefficient  $k_1 \approx -0.96$ . This property indicates that pseudo-critical point  $\lambda_m$  would approach asymptotically to the real critical point  $\lambda_c$  as the system size  $L \rightarrow \infty$  (e.g., higher  $n$ th RG). Moreover, the numerical results also indicate that  $d\mathcal{R}/d\lambda$  diverges logarithmically with the increasing size  $L$  as,

$$\frac{d\mathcal{R}}{d\lambda}|_{\lambda_m} = k_2 \ln L + const \quad (15)$$

at the pseudo-critical point  $\lambda_m$ . Here, coefficient  $k_2 \approx 1.00$ .

Now, we can investigate the finite-size scaling behavior. By taking into account the distance of the maximum of  $d\mathcal{R}/d\lambda$  from the critical point, we plot the value of

$$F = L^{-1}(\frac{d\mathcal{R}}{d\lambda} - \frac{d\mathcal{R}}{d\lambda}|_{\lambda_m}) \quad (16)$$

with respect to  $L^{1/\nu}(\lambda - \lambda_m)$  for different system size  $L$  (RG iteration rang from the 4rd iteration to the 7th one) in Fig.3. It is clearly that all the data collapse onto a single curve [27, 29]. Then we can get the critical exponent  $\nu = 1$ .

#### 4. EPR steering in XY chain

One-dimensional anisotropic XY spin chain is one of the fundamental models in the condensed many-body physics, the Hamiltonian is written as follows,

$$H(J, \gamma) = \frac{J}{4} \sum_i^L [(1 + \gamma)\sigma_x^i \sigma_x^{i+1} + (1 - \gamma)\sigma_y^i \sigma_y^{i+1}]. \quad (17)$$

Here,  $J$  and  $\gamma$  denote the coupling constant and the anisotropy parameter, respectively. This model can reduce to the XX one for  $\gamma = 0$  and the Ising one for  $\gamma = 1$ . According to the standard process of RG, the above Hamiltonian can be divided into the interblock and intrablock as follows [32, 33],

$$H_I^{BB} = \frac{J}{4} \sum_I^{L/3} [(1 + \gamma)\sigma_{3,I}^x \sigma_{1,I+1}^x + (1 - \gamma)\sigma_{3,I}^y \sigma_{1,I+1}^y] \\ H^B = \sum_I h_I^B. \quad (18)$$

Here,

$$h_I^B = \frac{J}{4} [(1 + \gamma)(\sigma_{1,I}^x \sigma_{2,I}^x + \sigma_{2,I}^x \sigma_{3,I}^x) \\ + (1 - \gamma)(\sigma_{1,I}^y \sigma_{2,I}^y + \sigma_{2,I}^y \sigma_{3,I}^y)] \quad (19)$$

is the three-site block Hamiltonian. Similarly, we can also easily obtain the two degeneracy ground state by solving the Schrödinger equation  $h_I^B|\phi\rangle = E|\phi\rangle$  as follows,

$$|\phi_0\rangle = \frac{1}{2\sqrt{1+\gamma^2}} (-\sqrt{1+\gamma^2}|\uparrow\uparrow\downarrow\rangle + \sqrt{2}|\uparrow\downarrow\uparrow\rangle \\ - \sqrt{1+\gamma^2}|\downarrow\uparrow\uparrow\rangle + \sqrt{2}\gamma|\downarrow\downarrow\downarrow\rangle) \quad (20)$$

$$|\phi'_0\rangle = \frac{1}{2\sqrt{1+\gamma^2}} (\sqrt{1+\gamma^2}|\downarrow\downarrow\uparrow\rangle - \sqrt{2}|\downarrow\uparrow\downarrow\rangle \\ + \sqrt{1+\gamma^2}|\uparrow\downarrow\downarrow\rangle - \sqrt{2}\gamma|\uparrow\uparrow\uparrow\rangle). \quad (21)$$

Then, by using the projection operator  $P_0$  for the  $I$ th block,

$$P_0^I = |\uparrow\uparrow\rangle_I \langle\phi_0| + |\downarrow\downarrow\rangle_I \langle\phi'_0|. \quad (22)$$

We can obtain the effective Hamiltonian as follows,

$$H^{eff} = \frac{J'}{4} \sum_i^L [(1 + \gamma')\sigma_x^i \sigma_x^{i+1} + (1 - \gamma')\sigma_y^i \sigma_y^{i+1}], \quad (23)$$

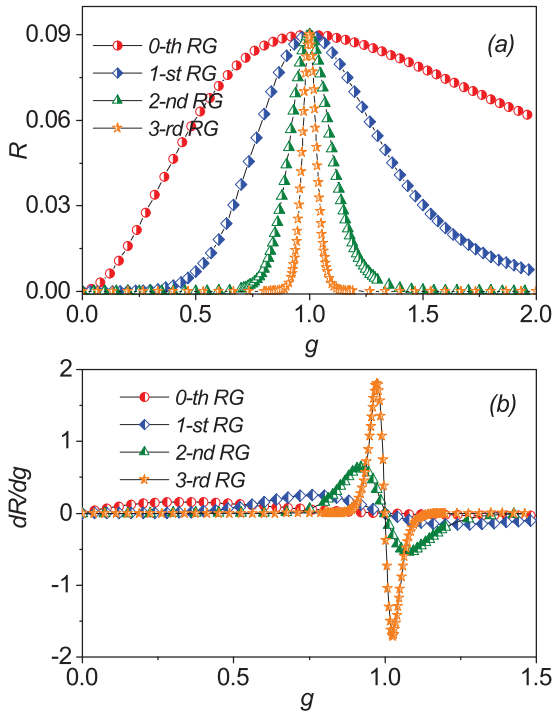


**Figure 4.** (Color online)(a) Steering robustness  $\mathcal{R}$  of the XY chain with respect to  $g$  under different RG steps. (b) Evolution of the first derivative of steering robustness  $d\mathcal{R}/dg$  under different RG steps.

which is also very similar with the original one. Here, the iterative relationship satisfy

$$J' = J \frac{3\gamma^2 + 1}{2(1 + \gamma^2)}, \quad \gamma' = \frac{\gamma^3 + 3\gamma}{3\gamma^2 + 1}. \quad (24)$$

Similarly, we can also obtain one stable fixed points ( $\gamma = \pm 1$ ) and one unstable fixed one ( $\gamma = 0$ ) by solving the above iterative relationship equation. Now, we can investigate EPR steering for the reduced mixed block state by taking account of the system size  $L$ . Here, we use  $|\phi_0\rangle$  to construct the density matrix which is defined by

$$\rho_{123} = |\phi_0\rangle\langle\phi_0|. \quad (25)$$

It should be mentioned that the result is the same if we consider the state  $|\phi'_0\rangle$ . By tracing out one of block spin in the quantum state  $\rho_{123}$  separately, we can derive the two-block spin reduced states as follows,

$$\rho_{13} = \text{tr}_2 \rho_{123} = \begin{pmatrix} \frac{1}{4}\Gamma^2 & 0 & 0 & \frac{\gamma}{4}\Gamma^2 \\ 0 & 1/4 & 1/4 & 0 \\ 0 & 1/4 & 1/4 & 0 \\ \frac{\gamma}{4}\Gamma^2 & 0 & 0 & \frac{\gamma^2}{4}\Gamma^2 \end{pmatrix}, \quad (26)$$

$$\rho_{23} = \text{tr}_1 \rho_{123} = \begin{pmatrix} \frac{1}{4} & 0 & 0 & -\frac{\gamma}{4}\Gamma \\ 0 & 1/4 & -\frac{1}{4}\Gamma & 0 \\ 0 & -\frac{1}{4}\Gamma & \frac{1}{4}\Gamma^2 & 0 \\ -\frac{\gamma}{4}\Gamma & 0 & 0 & \frac{\gamma^2}{2}\Gamma^2 \end{pmatrix}, \quad (27)$$

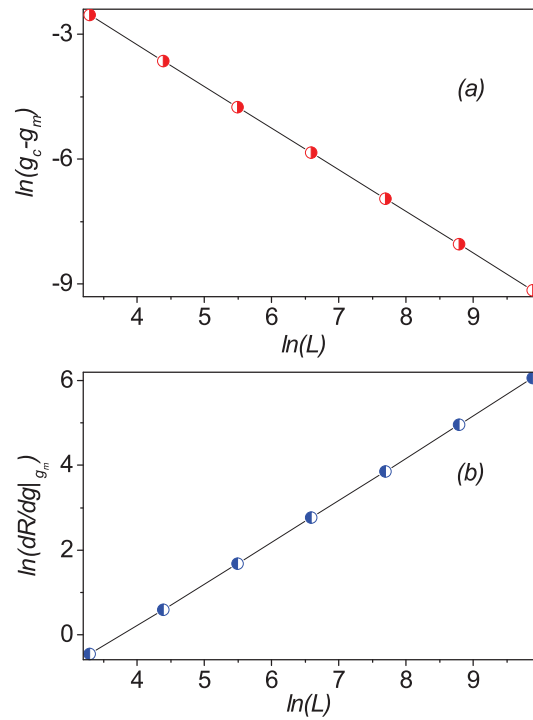


**Figure 5.** (Color online) (a) The distance between the position of pseudo-critical point  $g_m$  and the real one  $g_c$  with respect to different system size  $L$ .  $g_m$  approaches to  $g_c$  in terms of  $g_m = g_c + L^{-1.00}$ . (b) The minimum of the first derivative of steering robustness  $d\mathcal{R}/dg$  with respect to system size  $L$ . The minimum diverges as  $|d\mathcal{R}/dg|_{g_m} \sim L^{0.99 \pm 0.003}$ .

$$\rho_{12} = \text{tr}_3 \rho_{123} = \begin{pmatrix} \frac{1}{4} & 0 & 0 & -\frac{\gamma}{4}\Gamma \\ 0 & \frac{1}{4}\Gamma^2 & -\frac{1}{4}\Gamma & 0 \\ 0 & -\frac{1}{4}\Gamma & 1/4 & 0 \\ -\frac{\gamma}{4}\Gamma & 0 & 0 & \frac{\gamma^2}{2}\Gamma^2 \end{pmatrix} \quad (28)$$

with  $\Gamma = \sqrt{\frac{2}{1+\gamma^2}}$ . Obviously, the first one is the symmetric case, in which the steering robustness from block 1 to 3 (i.e. by measuring block 1) is equal to the case by measuring block 3. However, the second and third ones are the asymmetric case, which means that steering robustness may be different by measuring the middle block 2 or the corner block 1 (3). Interestingly, we find that the steering robustness for the reduced mixed block state  $\rho_{13} = \text{tr}_2 \rho_{123}$  remains zero for any  $\gamma$ , which means that  $\rho_{13}$  is not steerable despite the fact that there exists some other kinds of quantum correlations for this symmetry reduced mixed block state (e.g., entanglement [32], quantum discord, and measurement-induced disturbance [33]), so we only consider the latter case. Without loss of generality, we take  $\rho_{12}$  as an example in the following study.

Now, we can obtain the relationship between  $\mathcal{R}$  and  $\gamma$  in the reduced block state  $\rho_{12}$ . The renormalization of  $\gamma$  defines the evolution of the steering robustness  $\mathcal{R}$  with the increasing size of the system. To clarify the discussion of  $\mathcal{R}$  with respect to  $\gamma$ , we take the common approach by setting  $\mathcal{R}$  as a function of  $g$  in terms of  $g = (1 +$

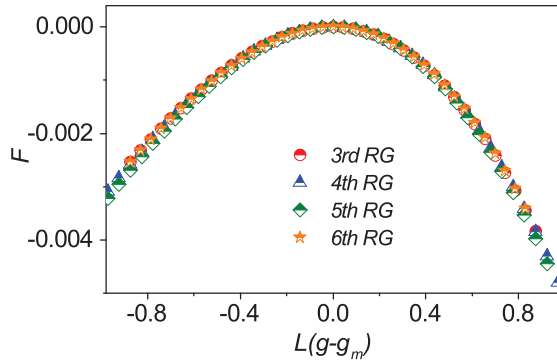


**Figure 6.** (Color online) The evaluated  $F = L^{-1}(\frac{dR}{dg} - \frac{dR}{dg}|_{g_m})$  with respect to  $L(g - g_m)$  for different RG steps  $n = 3, 4, 5$  and  $6$ . All the data almost collapse on a single curve.

$\gamma)/(1 - \gamma)$  [32, 33]. Fig.4(a) shows a plot of  $\mathcal{R}$  with respect to  $g$  under different RG iterations. Obviously, steering robustness  $\mathcal{R}$  also develops two fixed values in different region. At the critical point ( $g_c = 1$ ), steering robustness  $\mathcal{R}$  approaches to its maximum for all  $n$ th RG. In the other two regions  $0 \leq g < 1$  and  $g > 1$ ,  $\mathcal{R}$  approaches to zero asymptotically. Ma et al. have shown that the system is ferromagnetic order phase for  $g > 1$  and  $0 < g < 1$ , whilst the ground state of the system is characterized by a gapless excitation at the point  $g_c = 1$  ( $\gamma = 0$ ) [32].

To further reflect the trend of steering robustness with increasing system size  $L$  (i.e., higher  $n$ th RG), we also analyze the behavior of the first derivative of steering robustness  $d\mathcal{R}/dg$  as a function of  $g$ . The results are shown in Fig.4(b). Obviously,  $d\mathcal{R}/dg$  exhibits a sharp peak around both sides of the critical point  $g_c$ . In this work, we analyze the behavior of  $d\mathcal{R}/dg$  around the right side of the critical point  $g_c$ . The results are qualitatively similar by considering the behavior of  $d\mathcal{R}/dg$  around the left side of critical point. Obviously,  $d\mathcal{R}/d\lambda$  diverge around the critical point. Although there do not exit real divergence for a finite system size  $L$  (i.e., finite  $n$ th RG), the tend of such behavior become more obvious with increasing the lattice size, which indicate a the finite-size scaling behavior. Along this line, we can analyze the scaling behavior of  $d\mathcal{R}/dg|_{g_m}$  with respect to the size of system  $L$ . Here,  $g_m$  denotes the position of the minimum of  $d\mathcal{R}/dg$ . In the Fig.5 (a), we plot  $\ln|g_m - g_c|$  versus  $\ln(L)$ , which exhibits obviously a linear behavior  $\ln|g_m - g_c| \sim -\ln L$ . In other words, the position of pseudo-critical point  $g_m$  gradually tends to the real critical point  $g_c = 1$  as increasing system size  $L$ . Furthermore, the numerical calculation also indicate that  $d\mathcal{R}/dg$  diverges logarithmically with the increasing size  $L$  as,

$$\frac{d\mathcal{R}}{d\lambda}|_{\lambda_m} = k_2 \ln L + const \quad (29)$$

at the pseudo-critical point  $g_m$  (seeing Fig.5 (b)). Here, coefficient  $k_2 \approx 0.99 \pm 0.003$ . All these features state that steering robustness can also truly characterize the criticality of the  $XY$  model by the RG calculating.

We can also extract the critical exponent by investigating the finite-size scaling behavior. By taking into account the distance of the maximum of  $d\mathcal{R}/dg$  from the critical point, we plot the value of

$$F = L^{-1}(\frac{d\mathcal{R}}{dg} - \frac{d\mathcal{R}}{dg}|_{g_m}) \quad (30)$$

as a function of  $L^{1/\nu}(g - g_m)$  for different system size  $L$  (i.e.,  $n$ th RG) in Fig. 6. Here, the RG range from the 3rd iteration to the 6th one. Obviously, all these data almost collapse onto a single curve, which indeed indicate that the critical phenomena are scale invariant. And the critical exponent  $\nu = 1$  is obtained.

## 5. Asymmetry of EPR Steering

An interesting and inherent property of EPR steering, distinguishing it from both entanglement and Bell nonlocality, is its asymmetry between the two observers Alice and Bob [1]. This asymmetry feature contains two meanings. The first one is that the value of steerability may be different by measuring Alice's subsystem or Bob's ones. The second one is that steering may occur from Alice to Bob but not from Bob to Alice, or vice versa, for a given entangled state. Some previous works have paid extensive attention to this issue experimentally and theoretically [3, 9, 15, 16]. Here, it should be pointed out that such a phenomenon cannot occur for pure entangled states, which can always be brought to a symmetric form by changing the local basis. Hence, asymmetric quantum steering always requires mixed entangled states and the two observer's status should not be identical. Thereby this phenomenon will not emerge for the pure block state  $|\varphi_0\rangle$  in the ITF model, and we will only investigate such property for the reduced mixed block state in the anisotropic  $XY$  model.

From the above section, we know that the reduced block state  $\rho_{12}$  (or  $\rho_{23}$ ) in the block state  $\rho_{123}$  is asymmetric. Thereby it is both necessary and interesting to check the behavior of  $\mathcal{R}_{1 \rightarrow 2}$  (denoting the steering robustness from block 1 to 2) and  $\mathcal{R}_{2 \rightarrow 1}$  (denoting the steering robustness from block 2 to 1) with respect to  $g$  under different  $n$ th RG. In Fig.7, the behavior of  $\mathcal{R}_{1 \rightarrow 2}$  and  $\mathcal{R}_{2 \rightarrow 1}$  are plotted for a tridirectional measurement. Obviously, quantum steerability from block spin 2 to 1 ( $\mathcal{R}_{2 \rightarrow 1}$ ) is more robust than the steerability from block spin 1 to 2 ( $\mathcal{R}_{1 \rightarrow 2}$ ) in the reduced block state  $\rho_{12}$  for a given parameter  $g$ . This behavior indicates that quantum steering is asymmetric in such a quantum state, which is different from entanglement and Bell nonlocality. As a comparison, we also calculate steering robustness  $\mathcal{R}$  for the quantum state  $\rho_{12}$  by considering a bidirectional measurement. The results show that the quantum steering only occurs in the case of  $\mathcal{R}_{2 \rightarrow 1}$  for all  $g$  and  $n$ th RG, which means that quantum steering is one-way under such case.

From Fig.7, we know that  $\mathcal{R}_{1 \rightarrow 2}$  and  $\mathcal{R}_{2 \rightarrow 1}$  are not only different in their values for a fixed  $g$ , but also the points

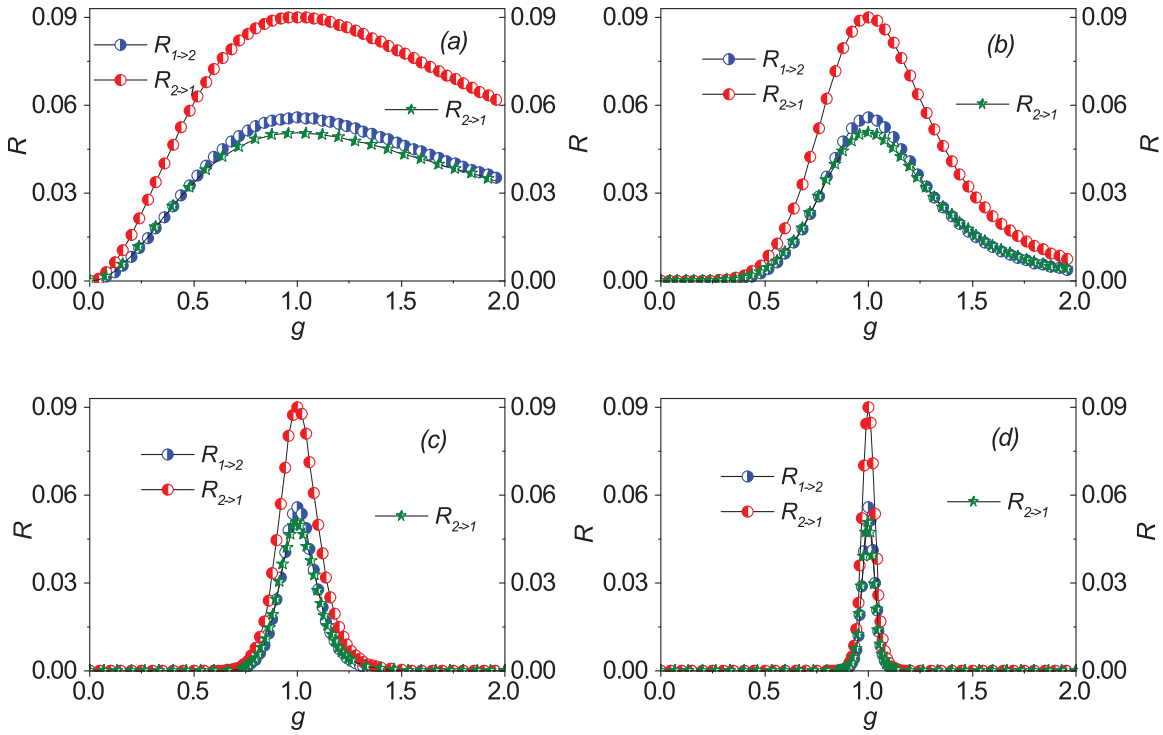


**Figure 7.** (Color online) Steering robustness  $\mathcal{R}$  of reduced mixed block state  $\rho_{12}$  in the XY model as a function of  $g$  with bidirectional-measurement (pentagram) and tridirectional measurement (circle) for different RG steps, respectively. (a) 0th, (b) 1st, (c) 2nd and (d) 3rd. For the bidirectional measurement, the plots show that the quantum steering can only occur in the case of measuring the middle block. For the tridirectional measurement, quantum steerability from middle-block to edge-block is more robust than the steerability from edge-block to the middle-block for a fixed parameter  $g$ .

**Table 1.** Threshold values  $g_{1(2) \rightarrow 2(1)}^*$  for which the reduced block state  $\rho_{12}$  is steerable from block 1 (2) to 2 (1) in the XY model with  $n$ th RG. Here,  $\Delta g^*$  denotes the gap between  $g_{2 \rightarrow 1}^*$  and  $g_{1 \rightarrow 2}^*$ .

$n$ th RG	3rd RG	4th RG	5th RG	6th RG	7th RG	8th RG	9th RG	10th RG	...
$g_{1 \rightarrow 2}^*$	0.727993	0.899586	0.965341	0.988311	0.996088	0.998694	0.9995646	0.9998548	...
$g_{2 \rightarrow 1}^*$	0.718706	0.895744	0.963965	0.987841	0.995930	0.998641	0.9995470	0.9998489	...
$\Delta g^*$	0.009287	0.003842	0.001376	0.000470	0.000158	0.000053	0.0000176	0.0000059	...

(noted by  $g^*$ ) where the steering emerges are also different for a given  $n$ th RG. To further understand the properties of asymmetry of the EPR steering, we study the system size scaling behavior. In Table 1, the positions of threshold values  $g_{1 \rightarrow 2}^*$  ( $g_{2 \rightarrow 1}^*$ ) and the gap  $\Delta g^* = g_{2 \rightarrow 1}^* - g_{1 \rightarrow 2}^*$  are displayed for different  $n$ th RG. It is obvious that the gap  $\Delta g^*$  approach zero with an increasing system size  $L$  (higher RG steps). In Fig.8, the logarithm of the gap  $\Delta g^*$ ,  $\ln(\Delta g^*)$  with respect to the logarithm of the system size  $\ln(L)$  ranging from the 4th RG to the 10th RG are presented, which shows a linear behavior between  $\ln(\Delta g^*)$  and  $\ln(L)$  as follows,

$$\ln(\Delta g^*) = k_3 \ln(L) + \text{const.} \quad (31)$$

with  $k_3 \simeq 0.99 \pm 0.005$ , which means that  $\Delta g^* \rightarrow 0$  as  $L \rightarrow \infty$ . In other words, there does not exist one-way EPR steering for a tridirectional-measurement under the limits  $L \rightarrow \infty$  despite the fact that EPR steering is asymmetric in the reduced block state  $\rho_{12}$ .

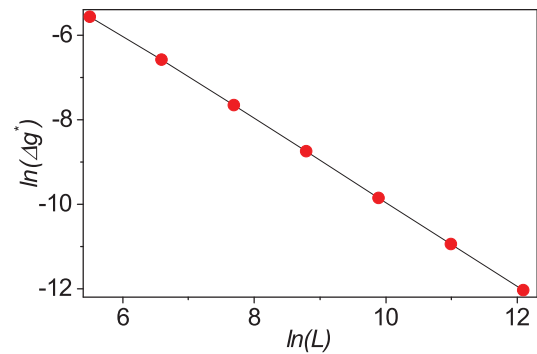


**Figure 8.** (Color online) The gap value  $g^*$  with respect to system size  $L$ , which shows a linear behavior as  $\ln(\Delta g^*) = 0.99 \ln(L) + \text{const.}$

## 6. summary

We have investigated the EPR steering for pure block state (two-site block in the ITF model) and reduced mixed block

state (three-site block in the  $XY$  model) by employing the quantum renormalization-group method. The results indicate that the first derivative of steering robustness show a divergent behavior, and obey finite-size scaling effect. Thus we can extract the critical exponent by calculation of steering robustness. All these features state that EPR steering can be as good as other quantum correlations (e.g. entanglement and Bell nonlocality) to detect the quantum phase transition in the two typical models.

Furthermore, the asymmetric feature of EPR steering, distinguishing it from both entanglement and Bell nonlocality, is also studied carefully for the reduced mixed block state  $\rho_{12}$  in the anisotropic  $XY$  model by both taking into account of measurement number and finite-size effect. For a bidirectional measurement, EPR steering can only exist by measuring the middle-block ( $\mathcal{R}_{2 \rightarrow 1}$ ). For a tridirectional measurement, quantum steerability from middle-block to edge-block ( $\mathcal{R}_{2 \rightarrow 1}$ ) is more robust than the steerability from edge-block to the middle-block ( $\mathcal{R}_{1 \rightarrow 2}$ ) in the reduced block state  $\rho_{12}$  for a given parameter  $g$ , which means that the quantum steering is asymmetric in such quantum state. To gain further insight, we also calculate the threshold values  $\delta_{1(2) \rightarrow 2(1)}^*$  and the gap  $\Delta g^*$  for different  $n$ th RG. The results state that the gap  $\Delta g^*$  approaches zero with increasing system size  $L$ . Moreover, the results also show that the logarithm of the gap  $\ln(\Delta g^*)$ , versus the logarithm of chain size  $\ln(L)$ , exhibits a linear behavior and thus shows a finite-size scaling effect. This behavior implies that one-way EPR steering does not exist in the reduced mixed block state  $\rho_{12}$  under the limits  $L \rightarrow \infty$  even if EPR steering is asymmetric for tridirectional measurement.

### Acknowledgments

Cheng is supported by the Jiangsu Government Scholarship for Overseas Studies and Science Foundation of Nanjing University of Posts and Telecommunication (Grant No. NY218005).

### References

- [1] Wiseman H M, Jones S J and Doherty A C 2007 *Phys. Rev. Lett.* **98** 140402.
- [2] Jones S J, Wiseman H M and Doherty A C 2007 *Phys. Rev. A* **76** 052116.
- [3] Händchen V, Eberle T, Steinlechner S, Samblowski A, Franz T, Werner R F and Schnabel R 2012 *Nature Photonics* **6** 596.
- [4] Reid M D, Drummond P D, Bowen W P, Cavalcanti E G, Lam P K, Bachor H A, Andersen U L and Leuchs G 2009 *Rev. Mod. Phys.* **81** 1727.
- [5] Skrzypczyk P, Navascués M and Cavalcanti D 2014 *Phys. Rev. Lett.* **112** 180404.
- [6] Cavalcanti D and Skrzypczyk P 2017 *Rep. Prog. Phys.* **80** 024001.
- [7] Pusey M F 2013 *Phys. Rev. A* **88** 032313.
- [8] Zhu H, Hayashi M and Chen L 2016 *Phys. Rev. Lett.* **116** 070403.
- [9] Bowles J, Vértesi T, Quintino M T and Brunner N 2014 *Phys. Rev. Lett.* **112** 200402.
- [10] Piani M and Watrous J 2015 *Phys. Rev. Lett.* **114** 060404.
- [11] Chen S L, Lambert N, Li C M, Miranowicz A, Chen Y N and Nori F 2016 *Phys. Rev. Lett.* **116** 020503.
- [12] Jevtic S, Pusey M, Jennings D and Rudolph T 2014 *Phys. Rev. Lett.* **113** 020402.
- [13] McCloskey R, Ferraro A and Paternostro M 2017 *Phys. Rev. A* **95** 012320.
- [14] Branciard C, Cavalcanti E G, Walborn S P, Scarani V and Wiseman H M 2012 *Phys. Rev. A* **85** 010301.
- [15] Sun K, Ye X J, Xu J S, Xu X Y, Tang J S, Wu Y C, Chen J L, Li C F and Guo G C 2016 *Phys. Rev. Lett.* **116** 160404.
- [16] Xiao Y, Ye X J, Sun K, Xu J S, Li C F and Guo G C 2017 *Phys. Rev. Lett.* **118** 140404.
- [17] Law Y Z, Thinh L P, Bancal J D and Scarani V 2014 *J. Phys. A: Math. Theor.* **47** 424028.
- [18] He Q, Rosales-Zárate L, Adesso G and Reid M D 2015 *Phys. Rev. Lett.* **115** 180502.
- [19] Reid M D 2013 *Phys. Rev. A* **88** 062108.
- [20] Bowles J, Hirsch F, Quintino M T and Brunner N 2016 *Phys. Rev. A* **93** 022121.
- [21] Uola R, Lever F, Gühne O and Pellonpää J P 2018 *Phys. Rev. A* **97** 032301.
- [22] Costa A C S and Angelo R M 2016 *Phys. Rev. A* **93** 020103.
- [23] Liu T H, Wang J C, Jing J L and Fan H 2018 *Ann. Phys.* **390** 334.
- [24] Cheng W W, Wang K, Wang W F and Guo Y J 2019 *J. Phys. B: At. Mol. Opt. Phys.* **52** 085501.
- [25] Sachdev S, *Quantum Phase Transition* (Cambridge University Press, Cambridge, England, 1997).
- [26] Amico L, Fazio R, Osterloh A and Vedral V 2008 *Rev. Mod. Phys.* **80** 517.
- [27] Osterloh A, Amico L, Falci G and Fazio R 2002 *Nature* **608** 416.
- [28] Osborne T J and Nielsen M A 2002 *Phys. Rev. A* **66** 032110.
- [29] Kargarian M, Jafari R and Langari A 2007 *Phys. Rev. A* **76** 060304.
- [30] Kargarian M, Jafari R and Langari A 2008 *Phys. Rev. A* **77** 032346.
- [31] Qin M, Ren Z Z and Zhang X 2016 *Sci. Rep.* **6** 26042.
- [32] Ma F W, Liu S X and Kong X M 2011 *Phys. Rev. A* **83** 062309.
- [33] Yao Y, Li H W, Zhang C M, Yin Z Q, Chen W, Guo G C and Han Z F 2012 *Phys. Rev. A* **86** 042102.
- [34] Batle J and Casas M 2010 *Phys. Rev. A* **82** 062101.
- [35] Justino L and de Oliveira T R 2012 *Phys. Rev. A* **85** 052128.
- [36] Song X K, Wu T, Xua S, He J and Ye L 2014 *Ann. Phys.* **349** 220.
- [37] Karpat G, Çakmak B and Fanchini F F 2014 *Phys. Rev. B* **90** 104431.
- [38] Altintas F and Eryigit R 2012 *Ann. Phys.* **327** 3084.
- [39] Sarandy M S 2009 *Phys. Rev. A* **80** 022108.